Angular distribution of the sputtered atoms from TbFeCo targets

Shiuh Chao, TzuanRen Jeng, VienShien Lo, DerRay Huang, and TsaiChu Hsiao

Citation: J. Appl. Phys. **74**, 5354 (1993); doi: 10.1063/1.354237

View online: http://dx.doi.org/10.1063/1.354237

View Table of Contents: http://jap.aip.org/resource/1/JAPIAU/v74/i9

Published by the American Institute of Physics.

Angular distribution of the sputtered atoms from TbFeCo targets

Shiuh Chao, Tzuan-Ren Jeng, and Vien-Shien Lo
Electronic Engineering Department, National Tsing Hua University, Hsin-Chu, Taiwan, Republic of China

Der-Ray Huang and Tsai-Chu Hsiao
Opto-Electronics and Systems Laboratory, Industrial Technology Research Institute, Hsin-Chu, Taiwan, Republic of China

(Received 19 October 1992; accepted for publication 20 July 1993)

The angular distribution of the sputtered Tb, Fe, and Co atoms from the elemental targets could be described by $\cos^n \theta$ distribution with $n=1.90$, 0.54, and 1.01 for Tb, Fe, and Co, respectively. For TbFeCo composite targets with mixed elemental and intermetallic compound phases, the overall angular distribution of the sputtered Tb, Fe, and Co atoms from the mixed phases could also be described by the $\cos^n \theta$ distribution function, and the values of the n's were related to the volume percentage of the intermetallic compound content in the composite target. This was not true of the Tb distribution for a target containing high intermetallic compound content. In that sample, an off-normal term has to be added to the $\cos^n \theta$ distribution function. It was found that a composite target with about 23 vol % intermetallic compound would produce a uniform composition distribution of TbFeCo film on the substrate.

I. INTRODUCTION

Magneto-optical (MO) disk storage technology employing the thermomagnetic effect for writing and erasing, and magneto-optical polar Kerr effect for reading, is now widely accepted for applications where high-storage density is required. Rare-earth–transition-metal (RE-TM) alloys are the most common material for MO recording thin films due to their good recording characteristics. Sputtering is the most appropriate means for preparing RE-TM thin films, since it may be easily integrated for mass production.

Sputtering of RE-TM alloy targets was reported to have problems by producing nonuniform composition distributions in the films on the disk.[1–3] The nonuniform composition distribution is mainly due to the different angular distribution of the sputtered atoms.[4] It was also reported[1–3] that the compositional uniformity in the film was related to the amount of intermetallic compound (IMC) phases presented in the RE-TM alloy sputter target.

For an ideal Knudson source, i.e., a source with random velocity distribution of the atom in the source and with a point opening, the angular distribution of the ejected atom is a cosine function. In sputtering process, factors such as ion energy, ion incident angle, target temperature, crystal structure, surface morphology, etc. deviate the angular distribution of the sputtered atoms from cosine distribution; for sputtering of a single-crystal target,[5] the angular distribution is concentrated along the crystallographic close-packed direction plus a cosine distribution about the surface normal; for sputtering of polycrystalline target, early work of Wehner and Rosenberg[6] showed that the angular distribution varied with the energy of the bombarding ion from "undercosine" to "cosine" and "overcosine" as the energy of bombarding Hg+ ion increased from 100 to 1000 eV and 20 keV for Ni and Pt targets. Since then, numerous results on the angular distribution of sputtered atoms from polycrystalline targets were reported. Many theoretical simulations of the sputtering process were started with the assumption of cosine function for the angular distribution.[7,8] Some models[9–11] used an ellipsoid normal to the surface for the angular distribution function. Here the ellipticity of the ellipsoid was adjusted to represent the condition of "overcosine" and "undercosine." We use an empirical function of cosine to the nth power for the angular distribution in this article. For n larger than one, the distribution is concentrated on the surface normal and is "oversine." For n smaller than one, the distribution is concentrated away from the surface normal and is "undercosine." We then calculate the mass distribution on the substrate for each element sputtered from a target based on the empirical angular distribution function of cosine to the nth power. The experimentally measured mass distribution of Tb, Fe, and Co on the substrate is then used to find the best-fit power of the cosine distribution for each kind of atom. Correlations among the power of cosine distribution and the amount of IMC phases content in the targets are then established. The adequacy of using the $\cos^n \theta$ function for various targets is also discussed.

II. MASS DISTRIBUTION IN THE FILM (REF. 12)

For a given target, the angular distribution of a certain kind of sputtered atom from a point on the target surface is designated as $F(\theta)$, referring to Fig. 1(a). The sputtered atomic mass flux dm in solid angle $d\Omega$ is given as

$$dm = AF(\theta)d\Omega, \tag{1}$$

with coefficient A determined by

$$\int_{\text{upper hemisphere}} dm = q, \tag{2}$$

where q is the total sputtered mass of a specific kind of atom from the point source. The total mass M of a specific

 0021-8979/93/74(9)/5354/6/$6.00

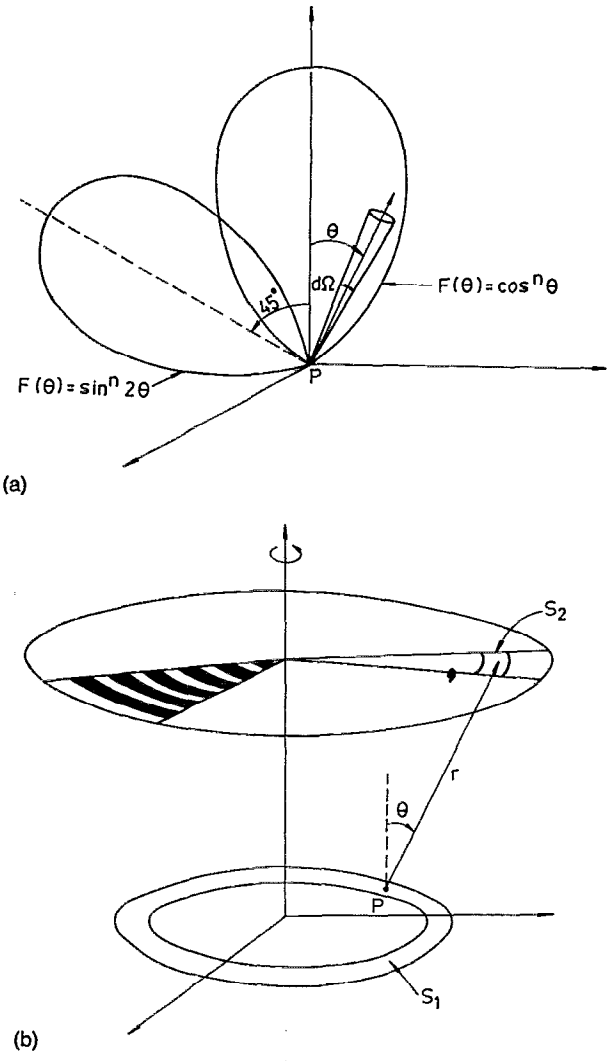

FIG. 1. (a) Angular distribution of the sputtered atom flux from a point source P for $\cos^n\theta$ and $\sin^n 2\theta$. (b) Relative position of the circular sputter source and the substrate. The shaded region in the fan-shaped area is exposed for deposition.

kind of atom impinging an area s_2 on the planar substrate from a sputter source of area s_1 is given as, referring to Fig. 1(b),

$$M=\int_{s_1}\int_{s_2} AF(\theta)\frac{\cos\theta}{r}\,ds_2\,ds_1. \tag{3}$$

The substrate is planar and parallel to the planar target.

For our experimental setup the sputter source is a circular magnetron, and the source area s_1 is therefore in a ring shape. The substrate is masked in a way such that only the shaded concentric stripe areas are exposed for deposition as shown in Fig. 1(b). The mass impinging each stripe can then be calculated from Eq. (3) for the setup in Fig. 1(b); the arithmetic and numerical processes are complicated but straightforward.[12]

We have assumed that the sticking coefficient to the substrate for each kind of atom is unity; then Eq. (3) gives the mass of the specific kind of atom in the film.

III. EXPERIMENT

We used five different sputter targets: elemental Tb, elemental Fe, elemental Co, $Tb_{26.6}Fe_{66.5}Co_{6.9}$ alloy with 35% (volume ratio) IMC, and $Tb_{24}Fe_{64.6}Co_{11.4}$ alloy with 100% IMC. The target with 35% IMC was prepared by a powder metallurgy method,[13] the target with 100% IMC was prepared by a melt-cast method.[14]

The sputtered apparatus was a circular dc magnetron unit, the disk substrate was parallel to the target, the center of the disk coincided with the center of the circular magnetron unit. The sputter targets were 2 in. in diameter, the circular magnetron was 2.5 cm in diameter, and the distance from the substrate to the target was 7 cm. The disk substrate was masked as shown in Fig. 1(b); only the shaded areas with a stripe on a fan-shaped region were exposed for deposition. The concentration of each kind of atom in the film per unit area of each stripe was measured by inductive coupled plasma atomic emission spectroscopy (ICP). The concentration per unit area of each stripe was then normalized to that of the first stripe which was closest to the center; therefore, the relative mass distribution per unit area of each kind of atom along the radial direction on the substrate was obtained.

If the dependence of the sticking coefficient on the angle of incidence is negligible in the range of 0°–45°, which was the largest angle from the sputter source to the substrate in our setup, then the validity of the assumption of unity sticking coefficient has no consequence on our results, since for each kind of atom the mass distribution was normalized, and the value of the sticking coefficient was thus canceled.

The dc magnetron sputter process was carried out in 5.5×10^{-3} torr argon pressure with 50 W dc sputter power, and the substrate was rotated at 30 rpm during deposition.

IV. RESULTS AND DISCUSSION

Four sets of samples were made for each kind of target, and the average value of relative mass distribution for these four samples was taken as the data point in Figs. 2–4. The measurement error of ICP was less than 1%, therefore, the error bar in these figures were mainly sample-to-sample variations. The sample-to-sample variations arise from the repositioning error of substrate for each deposition run.

A cosine to the nth power dependence is assumed for $F(\theta)$ as was discussed previously,

$$F(\theta)=\cos^n\theta.$$

Substituting $F(\theta)$ into Eq. (3) for our specific experimental setup, the empirical curve (solid curves in Figs. 2–4) of the relative mass distribution can be calculated. Figures 2, 3, and 4 show the experimental and best-fit empirical curves of relative mass distribution in films of Tb, Fe, and Co for the elemental targets and the targets containing 35% and 100% IMC, respectively. The inset figures in Figs. 2, 3, and 4 are the square error of fitting versus the value of n for Tb, Fe, and Co, respectively. The square error is defined as the square root of the sum of square of the difference between the experimental and the calculated

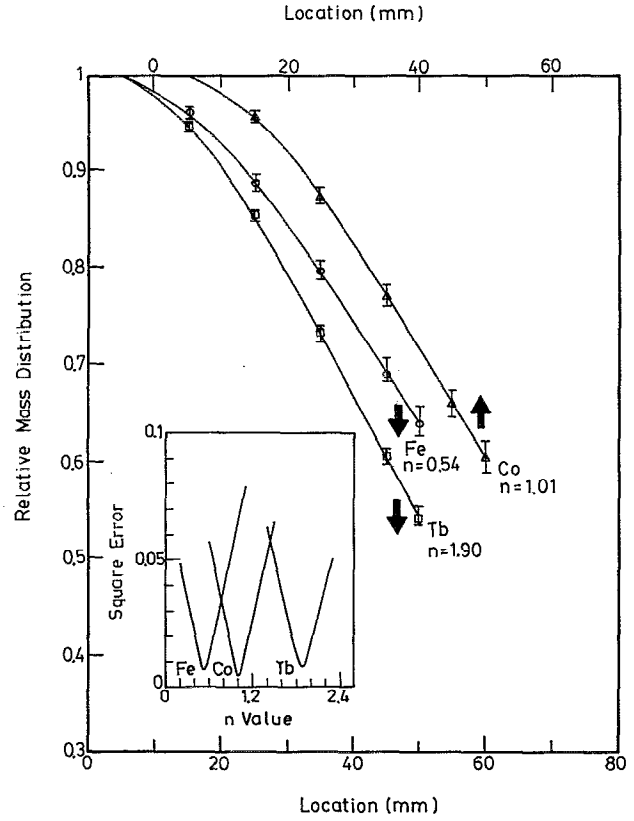

FIG. 2. The relative mass distribution per unit area along the radial direction of the substrate for Tb (□), Fe (○), and Co (△) sputtered from elemental target. Discrete points are experimental values, the solid curves are fitted curves. The inset is the square error of fitting vs the value of n of the $\cos^n \theta$ distribution.

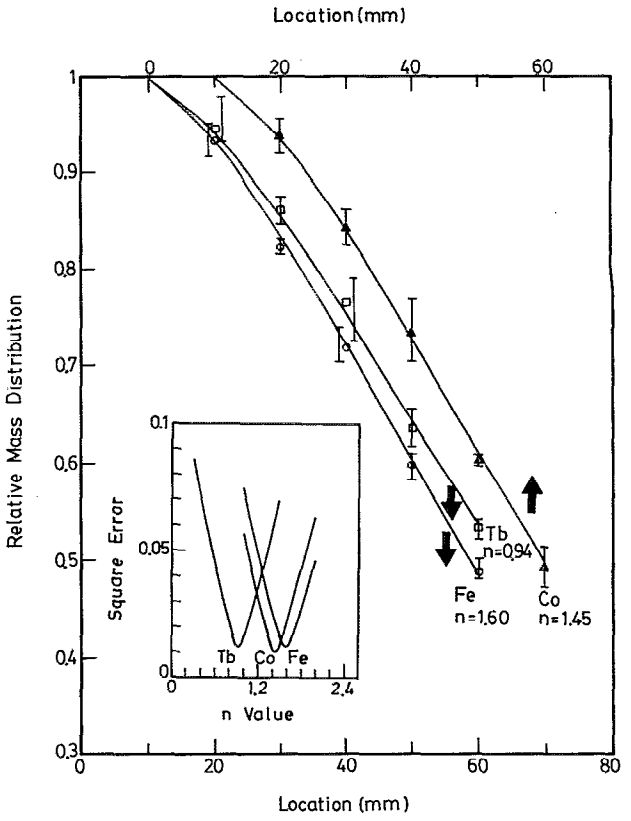

FIG. 3. Same as Fig. 2, but the sputtered target has 35% intermetallic compound content.

values of all data points. The uncertainty of determining of the value of n at the least-squares error was about ± 0.01. Table I lists the best-fit n values and the least-squares errors for all the cases.

In Fig. 4, the Tb distribution of the 100% IMC target cannot be fit by a simple $\cos^n \theta$ distribution, since it is above the $n=0$ curve as shown in the figure.

If the angular distribution of the sputtered atom is highly directed off the target surface normal as is shown in Fig. 1(a), mathematically a $\sin^n 2\theta$ term can be added to represent this off-normal component[15]:

$$F(\theta)=\cos^n \theta+\mathbf{a}\cdot\sin^{n_2} 2\theta.$$

Substituting this $F(\theta)$ into Eq. (3), the relative mass distribution for some numerical trials are shown in Fig. 5 for $n_1=0.1$, $n_2=1$, and the quantity **a** ranging from 0 to 2. Figure 5 demonstrates that in order to have a distribution curve above the $\cos^0 \theta$ curve as was the Tb curve in Fig. 4, the angular distribution function has to have an off-normal component such as $\sin^n 2\theta$. We can therefore conclude that the angular distribution of Tb atoms for the 100% IMC target cannot be simply described by a $\cos^n \theta$ distribution; rather, an off-normal component needs to be added.

The value of the least-squares error can serve as an indication of the degree of adequacy for the $\cos^n \theta$ function. From the insert figures of Figs. 2–4 and Table I, one can see that the $\cos^n \theta$ function fits the elemental targets and 35% IMC target better than the 100% IMC target.

It was reported[16] that during the sputtering process, surface segregation of Cu occurred at the surface of the Cu/Ni alloy target which caused Ni atoms to eject preferably in the direction of surface normal. It was also reported[17,18] that a concentration gradient which was produced at the binary target surface due to preferential sputtering would cause the sputtered atoms to eject in a preferred direction. These results implied that both the surface segregation of phases and concentration gradient caused by preferential sputtering could affect the angular distribution of the sputtered atoms in a complicated mechanism. For 100% IMC TbFeCo ternary alloy target, it was possible that some low-temperature phases might segregate on the target surface due to the heating by ion bombardment; it is also possible that some elements have a large sputtering yield compared to other elements in some phases producing a concentration gradient on the surface. These phenomena might then produce strong off-normal angular distribution for Tb, and mildly affect the Fe and Co distribution such that the $\cos^n \theta$ distribution applied less adequately to Fe and Co than pure elemental and 35% IMC targets. Detailed analysis of the microstructure of the 100% IMC target surface needs to be carried out in order to prove these assertions.

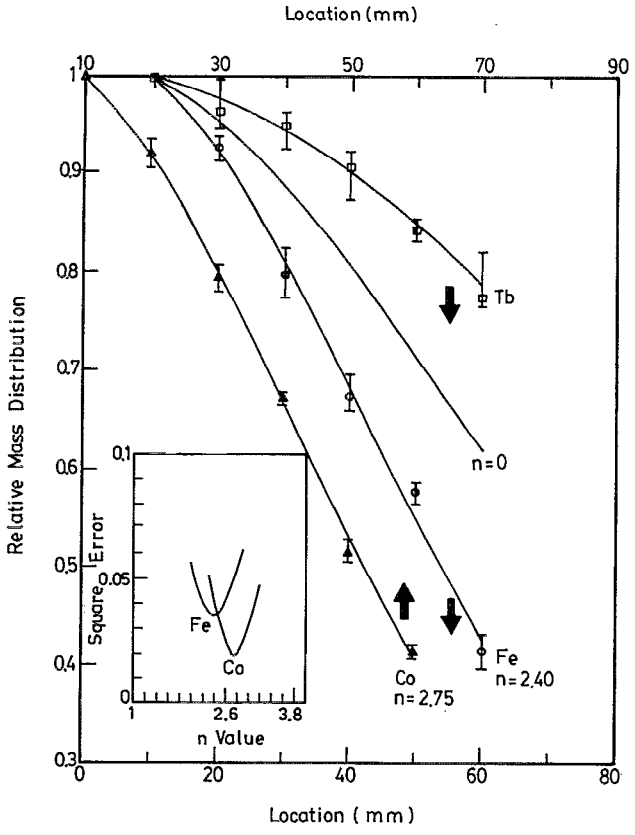

FIG. 4. Same as Fig. 2, but the sputtered target has 100% intermetallic compound content.

Table I indicates that the angular distribution of the sputtered Co atom changes from cosine ($n=1$) to overcosine ($n>1$) as the amount of IMC in the TbFeCo target increases. The angular distribution of sputtered Fe atoms changes from undercosine ($n<1$) to overcosine as the amount of IMC in the target increases. While the angular distribution of the sputtered Tb atoms changes, as the amount of IMC in the target increases, from overcosine to undercosine, and then changes to such an extent that an off-normal component in the distribution function appears. Figure 6 is the plot of the value of n's for $\cos^n\theta$ distribution versus the amount of intermetallic compound from Table I.

TABLE I. n values of $\cos^n\theta$ distribution function for Tb, Fe, and Co atoms sputtered from elemental, 35% intermetallic compound, and 100% intermetallic compound targets. Values in parentheses are the least-squares error of the fitting.

n of $\cos^n\theta$ (least-squares error)	Tb	Fe	Co
Elemental target	1.90 (0.0081)	0.54 (0.0066)	1.01 (0.0044)
35% intermetallic compound alloy target	0.94 (0.0121)	1.60 (0.0120)	1.45 (0.0098)
100% intermetallic compound alloy target	···	2.40 (0.0355)	2.75 (0.0187)

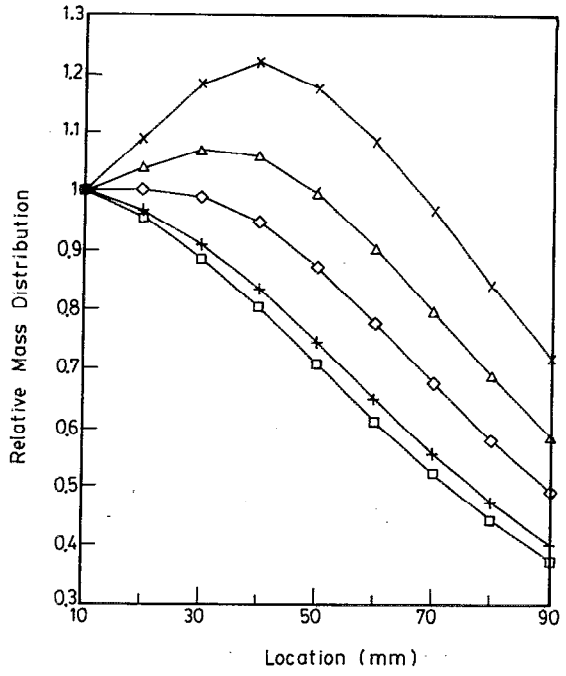

FIG. 5. Calculated curves for the relative mass distribution per unit area along the radial direction of the substrate for $F(\theta)=\cos^{0.1}\theta+\mathbf{a}\cdot\sin 2\theta$: $\mathbf{a}=0$ (□); $\mathbf{a}=0.1$ (+); $\mathbf{a}=0.5$ (◇); $\mathbf{a}=1.0$ (△); $\mathbf{a}=2.0$ (×).

For a uniform composition distribution of the film on the substrate to exist, it is required that the angular distribution of all the sputtered atoms be the same. Figure 6 indicates that at about 23% IMC content, the angular dis-

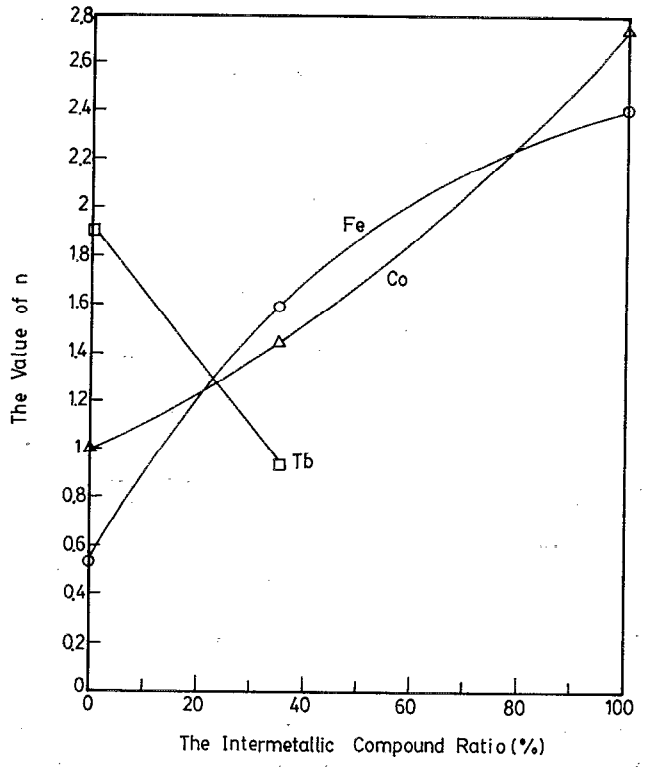

FIG. 6. The value of n for $\cos^n\theta$ distribution vs the amount of the intermetallic compound (vol %) in the target.

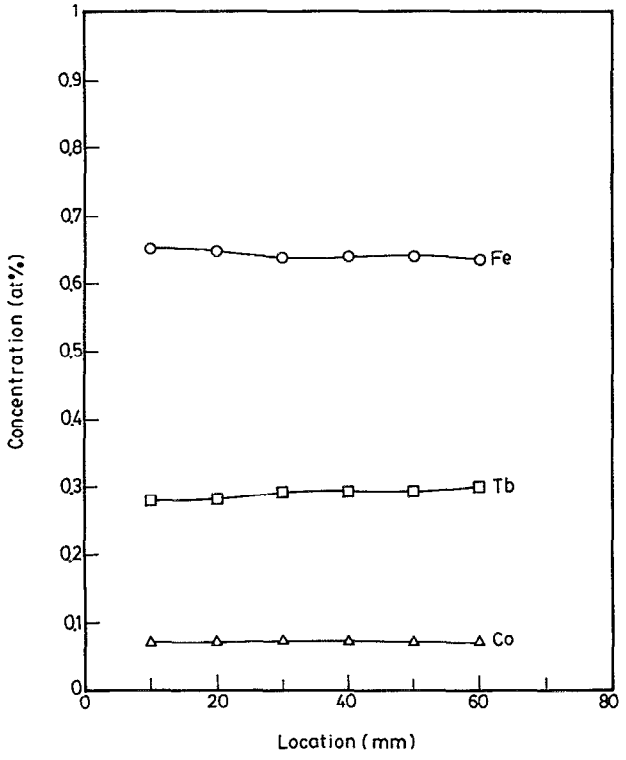

FIG. 7. The atomic concentration along the radial direction of the substrate for the film prepared by sputtering of a 35% intermetallic compound content $Tb_{26.6}Fe_{66.5}Co_{6.9}$ target.

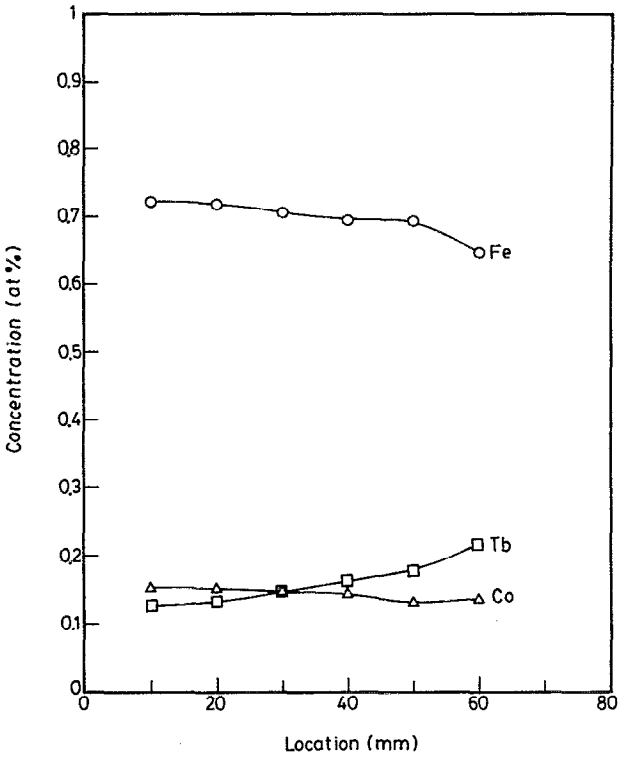

FIG. 8. The atomic concentration along the radial direction of the substrate for the film prepared by sputtering of a 100% intermetallic compound content $Tb_{24}Fe_{64.6}Co_{11.4}$ target.

tribution of sputtered Tb, Fe, and Co atoms is approximately the same, i.e., $\cos^{1.25}\theta$; therefore, with 23% IMC in the TbFeCo target, one would expect to obtain an uniform composition distribution of the film on the substrate. This finding is consistent with Schultheiβ's *et al.*[1] result: they used a 25% IMC target to produce a film with negligible composition gradient. Figures 7 and 8 show the atomic concentration of the TbFeCo films prepared by 35% IMC target and 100% IMC target, respectively. The concentration of the film prepared by the 35% IMC target is more uniform, and the concentration of the film is close to the concentration of the target, while the concentration of the film prepared by the 100% IMC target is less uniform and it seriously deviates from the concentration of the target in the area close to the substrate center.

One interesting point to notice is that the mean free path of Ar gas at 5.5×10^{-3} mbar is estimated to be 1.2 cm. Our substrate-to-target distance was 7 cm, and there were several collisions with Ar atoms on the way to the substrate for the sputtered atom. If the collisions randomized the angular distribution of the sputtered atoms to a great extent, then we would expect that there would be no difference of the observed angular distribution among different targets and atoms, and this is not true as is shown in Table I and Figs. 2–4. One possible explanation is that the average kinetic energy of the sputtered atoms is typically in the range of 1–20 eV,[19] while the average kinetic energy of the Ar atom at room temperature is $\frac{3}{2}$ kT($\sim$0.025 eV), the kinetic energy of the sputtered atoms is two to three orders of magnitude greater than the kinetic energy of the Ar atom, the Tb, Fe, and Co atoms are also heavier than the Ar atom; therefore, the momentum transfer during the collisions for randomizing the angular distribution is likely to be negligible.

The phase diagram of the TbFeCo ternary alloy system is not available in the literature, but one would expect that there must exist many different compound phases, both binary and ternary for the alloy system. For a given target with a certain amount of compound phases, there is no reason to expect that all the compound phases as well as the elemental phases would have the same angular distribution for a specific kind of sputtered atoms, but our results showed that, except for the Tb at high IMC content, the overall angular distribution for the sputtered atoms of the composite target can be properly described by an empirical $\cos^n\theta$ distribution function regardless of the fact that the distribution function for a specific kind of sputtered atom might be different among the individual phases.

V. CONCLUSION

We have made calculations for the composition distribution in a thin film with an empirical $\cos^n\theta$ angular distribution function for the sputtered atoms from the target.

By fitting the experimental results to the calculation, we found that the values of n for the $\cos^n \theta$ distribution are 1.90, 0.54, and 1.01 for Tb, Fe, and Co atoms sputtered from the elemental targets, respectively. For composite targets of TbFeCo with mixed phases of elemental and intermetallic compounds, although the angular distribution of a specific kind of atom may be different for each phase, we found that the overall angular distribution for each kind of atom from the composite target can also be adequately described by $\cos^n \theta$ for low-IMC-content targets. For high-IMC-content targets, the adequacy of $\cos^n \theta$ for Fe and Co is less than that of the low-IMC-content target, and an off-normal term is needed for the angular distribution function of Tb in particular. The surface concentration gradient caused by preferential sputtering and surface segregation of phases could have effects on the angular distribution of the sputtered atoms of high-IMC-content targets. The power n of the $\cos^n \theta$ distribution increases for Fe and Co, and decreases for Tb as the amount of IMC phases in the target increases. The crossover point is $\cos^{1.25} \theta$ for 23% IMC content, which means that for the TbFeCo target with 23% IMC content a uniform composition distribution of the film on the substrate can be obtained.

[1] E. Schultheiß, G. Brauer, P. Wirz, St. U. Schittny, L. A. Berchthold, and H.-P. D. Shieh, IEEE Trans. Magn. **MAG-24**, 2772 (1988).
[2] Y. Murakami, T. Shingyoji, and K. Hizikata, J. Vac. Sci. Technol. A **8**, 7 (1990).
[3] Y. Murakami, T. Shingyoji, and K. Hizikata, J. Appl. Phys. **68**, 1866 (1990).
[4] R. R. Olson and G. K. Webner, J. Vac. Sci. Technol. **14**, 319 (1977).
[5] R. G. Musket and H. P. Smith, Jr., J. Appl. Phys. **39**, 3579 (1968).
[6] G. K. Wehner and D. Rosenberg, J. Appl. Phys. **3**, 177 (1960).
[7] R. J. Gnaedinger, Jr., J. Vac. Sci. Technol. **6**, 355 (1969).
[8] G. C. Schwartz, R. E. Jones, and L. I. Maissel, J. Vac. Sci. Technol. **6**, 351 (1969).
[9] I. A. Blech and H. A. Vander Plas, J. Appl. Phys. **54**, 3489 (1983).
[10] C. E. Wickersbam, Jr., J. Vac. Sci. Technol. A **5**, 1755 (1987).
[11] H. Tsuge, S. Esho, and H. Gokan, J. Vac. Sci. Technol. **19**, 221 (1981).
[12] V. S. Lo, Master thesis, National Tsing Hua University, 1992.
[13] Mitsubishi Materials Corporation, Japan.
[14] Mitsui Engineering and Shipbuilding Co., Ltd., Advance Materials and Product, Japan.
[15] T. Motohiro, J. Vac. Sci. Technol. A **4**, 189 (1986).
[16] S. Ichimura, H. Shimizu, and H. Murakami, J. Nucl. Mater. **128 & 129**, 601 (1984).
[17] H. H. Anderson, B. Stenum, T. Sorensen, and H. J. Whitlow, Nucl. Instrum. Methods **209/210**, 487 (1983).
[18] H. J. Kang, Y. Matsuda, and R. Shimizu, Surf. Sci. **127**, L179 (1983).
[19] G. K. Wehner and G. S. Anderson, in *Handbook of Thin Film Technology*, edited by L. I. Maissel and R. Glang (McGraw-Hill, New York, 1970), Chap. 3.